

Oscillatory Hartmann Flow in a Rotating Channel with Magnetized Walls

G. S. Seth¹, J. K. Singh^{2,*}, N. Mahto³ and N. Joshi²

¹ Department of Applied Mathematics, Indian School of Mines, Dhanbad-826004, India.

² Department of Mathematics, V. S. K. University, Bellary-583105, India

³ Department of Mathematics, R. S. P. College Jharia, Dhanbad, India

Received: 5 Jan. 2016, Revised: 20 Mar. 2016, Accepted: 23 Mar. 2016

Published online: 1 Sep. 2016

Abstract: Oscillatory Hartmann flow of a viscous, incompressible and electrically conducting fluid in a rotating channel with magnetized walls in the presence of a uniform transverse magnetic field is studied. Exact solution of the governing equations is obtained in closed form. Mathematical formulation of the problem contains four pertinent flow parameters, namely, magnetic parameter α_m , Ekman number E , frequency parameter ω and magnetic Prandtl number P_m . Solutions in the limit of vanishing magnetic Prandtl number P_m and small finite magnetic Prandtl number P_m are also obtained. Asymptotic behavior of these solutions is analyzed for large values of frequency parameter ω to gain some physical insight into the flow pattern. Expressions for the shear stress at the plates due to primary and secondary flows and mass flow rates in the primary and secondary flow directions are also derived. The numerical values of the fluid velocity and induced magnetic field are displayed graphically whereas that of shear stress at the plates due to primary and secondary flows and mass flow rates in the primary and secondary flow directions are presented in tabular form for various values of α_m^2 and ω .

Keywords: Rotation, magnetic field, oscillations, hydromagnetic Stokes-Ekman boundary layers.

1 Introduction

Theoretical/experimental investigation of magnetohydrodynamic flow of an electrically conducting fluid assumes considerable importance due to occurrence of various natural phenomena which are generated by the action of Coriolis and magnetic forces. It is widely accepted that the Coriolis force has considerable influence on hydromagnetic flow in Earth's liquid core. A large number of astronomical bodies (i.e. Sun, Earth, Jupiter, magnetic stars and pulsars) possess fluid interiors and (at least surface) magnetic field. In addition to its application in geophysical and astrophysical problems of interest, such studies may find applications in various areas of science and technology e.g. turbo machines, vortex type MHD power generators, nuclear reactors using liquid metal coolant, material processing etc. Keeping in view the importance of such studies a number of research investigations of hydromagnetic flow in a rotating medium are carried out during past few decades by many researchers. Mention may be made of research works of

Hide and Roberts [1], Nanda and Mohanty [2], Gupta [3], Acheson [4], Seth and Jana [5], Sarojamma and Krishna [6], Seth *et al.* [7,8,9,10,11,12], Seth and Ghosh [13], Raptis and Singh [14], Nanousis [15], Chandran *et al.* [16], Singh *et al.* [17], Nagy and Demendy [18], Singh [19], Hayat *et al.* [20,21,22,23], Ghosh and Pop [24,25], Ghosh *et al.* [26], Guria *et al.* [27], Das *et al.* [28] and Chauhan and Agrawal [29]. It may be noted that the fluid transient may be expected in many MHD devices, namely, MHD energy generators, MHD pumps, induction type pumps used in nuclear reactors, MHD flow meters, MHD accelerators etc. Keeping in view the importance of such phenomena Seth and Jana [5], Sarojamma and Krishna [6], Seth *et al.* [7,8,9,10,11,12], Seth and Ghosh [13], Chandran *et al.* [16], Singh *et al.* [17], Singh [19], Hayat *et al.* [20,21,22,23], Guria *et al.* [27] and Das *et al.* [28] studied unsteady hydromagnetic flow of a viscous, incompressible and electrically conducting fluid in a rotating system considering different aspects of the problem. In all these investigations induced magnetic field generated by fluid motion is neglected in comparison

* Corresponding author e-mail: s.jitendrak@yahoo.com

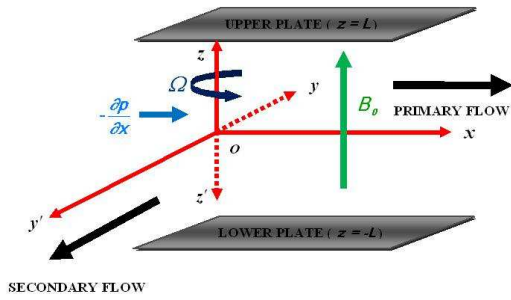


Fig. 1: Physical Model of the problem

to the applied one. This assumption is valid because magnetic Reynolds number is very small for liquid metals and slightly ionized fluids (Cramer and Pai [30]). However, for the problems of astrophysical and geophysical interest magnetic Reynolds number is not very small. Therefore, induced magnetic field plays a significant role in determining the flow patterns of such fluid flow problems. Taking into consideration this fact Ghosh [31], Seth *et al.* [32] and Ansari *et al.* [33] considered oscillatory hydromagnetic flow of a viscous, incompressible and electrically conducting fluid in a rotating channel under different conditions taking induced magnetic field into account.

The purpose of the present study is to investigate oscillatory hydromagnetic flow of a viscous, incompressible and electrically conducting fluid in a rotating channel with magnetized walls in the presence of a uniform transverse magnetic field. Fluid flow within the channel is induced due to an oscillating pressure gradient applied along the channel walls.

2 Mathematical Analysis

Consider oscillatory flow of a viscous, incompressible and electrically conducting fluid within a parallel plate channel $z = \pm L$ in the presence of a uniform transverse magnetic field B_0 which is applied parallel to z -axis. Both the fluid and channel rotate in unison in a counter clockwise direction with a uniform angular velocity Ω about z -axis. Fluid flow within the channel is induced due to a periodic pressure gradient $-\frac{\partial p}{\partial x} = R'_1 \cos \omega't$ which is applied in x -direction. R'_1, ω', t and p are amplitude, frequency of oscillations, time and modified pressure including centrifugal force respectively. Physical model of the problem is presented in figure-1. Since plates of the channel are of infinite extent in x and y -directions, all physical quantities except pressure depend on z and t only.

Fluid velocity \vec{q} and induced magnetic field \vec{B} are given by

$$\vec{q} \equiv (u', v', 0) \quad \text{and} \quad \vec{B} \equiv (B'_x, B'_y, B_0). \tag{1}$$

These assumptions are in agreement with the fundamental equations of MHD in a rotating frame of reference.

Under the above assumptions the governing equations for flow of a viscous, incompressible and electrically conducting fluid in a rotating system are given by

$$\frac{\partial u'}{\partial t} - 2\Omega v' = -\frac{1}{\rho} \frac{\partial p}{\partial x} + \nu \frac{\partial^2 u'}{\partial z^2} + \frac{B_0}{\rho \mu_e} \frac{\partial B'_x}{\partial z}, \tag{2}$$

$$\frac{\partial v'}{\partial t} + 2\Omega u' = \nu \frac{\partial^2 v'}{\partial z^2} + \frac{B_0}{\rho \mu_e} \frac{\partial B'_y}{\partial z}, \tag{3}$$

$$0 = -\frac{1}{\rho} \frac{\partial}{\partial z} \left\{ p + \frac{1}{2\mu} (B_x'^2 + B_y'^2 + B_0^2) \right\}, \tag{4}$$

$$\frac{\partial B'_x}{\partial t} = B_0 \frac{\partial u'}{\partial z} + \nu_m \frac{\partial^2 B'_x}{\partial z^2}, \tag{5}$$

$$\frac{\partial B'_y}{\partial t} = B_0 \frac{\partial v'}{\partial z} + \nu_m \frac{\partial^2 B'_y}{\partial z^2}, \tag{6}$$

where ρ, ν, μ_e and ν_m are, respectively, fluid density, kinematic coefficient of viscosity, magnetic permeability and magnetic viscosity of the fluid.

Equation (4) shows the constancy of the modified pressure along z -axis i.e. axis of rotation. There is a net cross flow in y -direction so the pressure gradient term $\frac{\partial p}{\partial y}$ is not taken into account in equation (3).

Since plates of the channel are assumed magnetized, boundary conditions for the velocity and induced magnetic fields are

$$\begin{cases} u' = v' = 0 & \text{at } z = \pm L, \\ B'_x = \frac{R'_1}{2} (e^{i\omega't} + e^{-i\omega't}), \\ B'_y = 0 & \text{at } z = \pm L. \end{cases} \tag{7}$$

Introducing non-dimensional variables $x = \xi L, z = \eta L, u' = \Omega L u, v' = \Omega L v, B'_x = \sigma \mu_e B_0 L (\nu \Omega)^{\frac{1}{2}} B_x, B'_y = \sigma \mu_e B_0 L (\nu \Omega)^{\frac{1}{2}} B_y, T = \Omega t$ and $p = \rho \Omega^2 L^2 p^*$, the equations (2), (3), (5) and (6), in non-dimensional form, become

$$\frac{\partial u}{\partial T} - 2v = -\frac{\partial p^*}{\partial \xi} + E \frac{\partial^2 u}{\partial \eta^2} + 2\alpha_m^2 E^{\frac{1}{2}} \frac{\partial B_x}{\partial \eta}, \tag{8}$$

$$\frac{\partial v}{\partial T} + 2u = E \frac{\partial^2 v}{\partial \eta^2} + 2\alpha_m^2 E^{\frac{1}{2}} \frac{\partial B_y}{\partial \eta}, \tag{9}$$

$$P_m \frac{\partial B_x}{\partial T} = E^{\frac{1}{2}} \frac{\partial u}{\partial \eta} + E \frac{\partial^2 B_x}{\partial \eta^2}, \tag{10}$$

$$P_m \frac{\partial B_y}{\partial T} = E^{\frac{1}{2}} \frac{\partial v}{\partial \eta} + E \frac{\partial^2 B_y}{\partial \eta^2}, \tag{11}$$

where $E = \frac{\nu}{\Omega L^2}$ is the Ekman number, $P_m = \frac{\nu}{v_m} = \sigma \mu_e \nu$ is the magnetic Prandl number and $\alpha_m = \frac{dE}{\sqrt{2}dH} = \left(\frac{\sigma}{2\rho\Omega}\right)^{\frac{1}{2}} B_0$ is the magnetic interaction parameter.

Since $dE = \left(\frac{\nu}{\Omega}\right)^{\frac{1}{2}}$ is the Ekman depth and $dH = \left(\frac{\rho\nu}{\sigma B_0^2}\right)^{\frac{1}{2}}$ is the Hartmann depth, therefore, their ratio given by $\sqrt{2}\alpha_m$ is the ratio of Ekman and Hartmann depths. This ratio is independent of viscosity and from its position in equations (8) and (9), $2\alpha_m^2$ measures the strength of electromagnetic body force relative to Coriolis force. Also for physical situations of interest both E and P_m are smaller than unity.

The boundary conditions (7), in non-dimensional form, become

$$\begin{cases} u = v = 0 & \text{at } \eta = \pm 1, \\ B_x = \frac{R}{2}(e^{i\omega T} + e^{-i\omega T}), \\ B_y = 0 & \text{at } \eta = \pm 1, \end{cases} \quad (12)$$

where $R = \frac{R'}{\sigma \mu_e (\nu \Omega)^{\frac{1}{2}} B_0 L}$ is a non-dimensional constant and $\omega = \frac{\omega'}{\Omega}$ is frequency parameter.

Combining equations (8) and (10) with equations (9) and (11) respectively, we obtain

$$\begin{cases} \frac{\partial F}{\partial T} + 2iF = -\frac{\partial p^*}{\partial \xi} \\ + E \frac{\partial^2 F}{\partial \eta^2} + 2\alpha_m^2 \alpha E^{\frac{1}{2}} \frac{\partial b}{\partial \eta}, \end{cases} \quad (13)$$

$$P_m \frac{\partial b}{\partial T} = E^{\frac{1}{2}} \frac{\partial F}{\partial \eta} + E \frac{\partial^2 b}{\partial \eta^2}, \quad (14)$$

where $F = u + iv$ and $b = B_x + iB_y$.

Boundary conditions (12), in compact form, become

$$\begin{cases} F(\eta, T) = 0 & \text{at } \eta = \pm 1, \\ b(\eta, T) = \frac{R}{2}(e^{i\omega T} + e^{-i\omega T}) \\ \text{at } \eta = \pm 1. \end{cases} \quad (15)$$

Since the fluid flow within the channel is induced due to oscillatory pressure gradient applied in x-direction, the pressure gradient term $-\left(\frac{\partial p^*}{\partial \xi}\right)$, fluid velocity $F(\eta, T)$ and induced magnetic field $b(\eta, T)$ are assumed in the following form

$$-\frac{\partial p^*}{\partial \xi} = \frac{R_1}{2}(e^{i\omega T} + e^{-i\omega T}), \quad (16)$$

$$F(\eta, T) = F_1(\eta)e^{i\omega T} + F_2(\eta)e^{-i\omega T}, \quad (17)$$

$$b(\eta, T) = b_1(\eta)e^{i\omega T} + b_2(\eta)e^{-i\omega T}, \quad (18)$$

where $R_1 = \frac{R'}{\rho \Omega^2 L}$ is non-dimensional constant.

Using equations (16) to (18) in equations (13) and (14), we obtain

$$E \frac{d^2 F_1}{d\eta^2} - i(\omega + 2)F_1 = -2\alpha_m^2 E^{\frac{1}{2}} \frac{db_1}{d\eta} - \frac{R_1}{2}, \quad (19)$$

$$E \frac{d^2 F_2}{d\eta^2} + i(\omega - 2)F_2 = -2\alpha_m^2 E^{\frac{1}{2}} \frac{db_2}{d\eta} - \frac{R_1}{2}, \quad (20)$$

$$E \frac{d^2 b_1}{d\eta^2} - i\omega P_m b_1 = -E^{\frac{1}{2}} \frac{dF_1}{d\eta}, \quad (21)$$

$$E \frac{d^2 b_2}{d\eta^2} + i\omega P_m b_2 = -E^{\frac{1}{2}} \frac{dF_2}{d\eta}. \quad (22)$$

The boundary conditions (15) with the help of (17) and (18) reduce to

$$\begin{cases} F_1 = F_2 = 0 & \text{at } \eta = \pm 1, \\ b_1 = b_2 = \frac{R}{2} & \text{at } \eta = \pm 1. \end{cases} \quad (23)$$

Solving equations (19) to (22) subject to the boundary conditions (23), we obtain the solution for velocity and induced magnetic field which are presented in the following form

$$\begin{aligned} F(\eta, T) = & -\frac{i}{2(\omega+2)} [R_1 \{C_1 (\cosh \alpha_1 \eta \\ & - \frac{\cosh \alpha_1}{\cosh \alpha_2} \cosh \alpha_2 \eta) \\ & + (1 - \frac{\cosh \alpha_2 \eta}{\cosh \alpha_2})\} \\ & + RC_2 (\sinh \alpha_1 \eta \\ & - \frac{\sinh \alpha_1}{\sinh \alpha_2} \sinh \alpha_2 \eta)] e^{i\omega T} \\ & + \frac{i}{2(\omega-2)} [R_1 \{a_1 (\cosh \beta_1 \eta \\ & - \frac{\cosh \beta_1}{\cosh \beta_2} \cosh \beta_2 \eta) \\ & + (1 - \frac{\cosh \beta_2 \eta}{\cosh \beta_2})\} \\ & + Ra_2 (\sinh \beta_1 \eta \\ & - \frac{\sinh \beta_1}{\sinh \beta_2} \sinh \beta_2 \eta)] e^{-i\omega T}, \end{aligned} \quad (24)$$

$$\begin{aligned} b(\eta, T) = & R_2 [R_1 \{C_1 \{k_1^* \sinh \alpha_1 \eta \\ & - m_1^* \frac{\cosh \alpha_1}{\cosh \alpha_2} \sinh \alpha_2 \eta\} - m_1^* \frac{\sinh \alpha_2 \eta}{\cosh \alpha_2}\} \\ & + RC_2 \{k_1^* \cosh \alpha_1 \eta - m_1^* \frac{\sinh \alpha_1}{\sinh \alpha_2} \cosh \alpha_2 \eta\}] e^{i\omega T} \\ & + R_3 [R_1 \{a_1 \{k_3^* \sinh \beta_1 \eta - m_2^* \frac{\cosh \beta_1}{\cosh \beta_2} \sinh \beta_2 \eta\} \\ & - m_3^* \frac{\sinh \beta_2 \eta}{\cosh \beta_2}\} + Ra_2 \{k_2^* \cosh \beta_1 \eta \\ & - m_3^* \frac{\sinh \beta_1}{\sinh \beta_2} \cosh \beta_2 \eta\}] e^{-i\omega T}, \end{aligned} \quad (25)$$

where

$$\begin{cases}
 R_2 = 1/4\omega(\omega + 2) \cdot P_m \alpha_m^2, \\
 R_3 = 1/4\omega(\omega - 2) \cdot P_m \alpha_m^2, \\
 n_1 = \frac{1}{2}[2\alpha_m^2 + i\{\omega(1 + P_m) + 2\}], \\
 n_2 = \frac{1}{2}[2\alpha_m^2 - i\{\omega(1 + P_m) - 2\}], \\
 q_1 = i\{\omega(\omega + 2)P_m\}^{\frac{1}{2}}, \\
 q_2 = i\{\omega(\omega - 2)P_m\}^{\frac{1}{2}}, \\
 k_1, m_1 = [n_1 \pm (n_1^2 - q_1^2)^{1/2}]^{1/2}, \\
 k_2, m_2 = [n_2 \pm (n_2^2 - q_2^2)^{1/2}]^{1/2}, \\
 \alpha_1, \alpha_2 = E^{-1/2}(k_1, m_1), \\
 \beta_1, \beta_2 = E^{-1/2}(k_2, m_2), \\
 \alpha^* = \{2\alpha_m^2 + i(\omega + 2)\}^{1/2}, \\
 \beta^* = \{2\alpha_m^2 - i(\omega - 2)\}^{1/2}, \\
 k_1^* = k_1(k_1^2 - \alpha^{*2}), m_1^* = m_1(m_1^2 - \alpha^{*2}), \\
 k_2^* = k_2(k_2^2 - \alpha^{*2}), m_2^* = m_2(m_2^2 - \alpha^{*2}), \\
 k_3^* = k_2(k_2^2 - \beta^{*2}), m_3^* = m_2(m_2^2 - \beta^{*2}), \\
 C_1 = \frac{m_1^* \tanh \alpha_2}{k_1^* \sinh \alpha_1 - m_1^* \cosh \alpha_1 \tanh \alpha_2}, \\
 C_2 = \frac{2\omega(\omega + 2)P_m \alpha_m^2}{k_1^* \cosh \alpha_1 - m_1^* \sinh \alpha_1 \coth \alpha_2}, \\
 a_1 = \frac{m_1^* \tanh \beta_2}{k_2^* \sinh \beta_1 - m_2^* \cosh \beta_1 \tanh \beta_2}, \\
 a_2 = \frac{2\omega(\omega - 2)P_m \alpha_m^2}{k_2^* \cosh \beta_1 - m_2^* \sinh \beta_1 \coth \beta_2}.
 \end{cases} \tag{26}$$

We shall now discuss some particular cases of interest of the general solution (24) to (26) to gain some physical insight into flow pattern.

Case-I: Oscillatory Hydromagnetic Flow in the Limit of Vanishing Magnetic Prandtl number (i.e. $P_m \rightarrow 0$)

When $P_m \rightarrow 0$ in equations (24) to (26), we obtain

$$\begin{cases}
 n_1 = \frac{1}{2}[2\alpha_m^2 + i(\omega + 2)], \\
 n_2 = \frac{1}{2}[2\alpha_m^2 - i(\omega - 2)], \\
 q_1 \rightarrow 0, q_2 \rightarrow 0, \\
 m_1 \rightarrow 0, m_2 \rightarrow 0, \\
 k_1 = (n_1)^{1/2}, k_2 = (n_2)^{1/2},
 \end{cases} \tag{27}$$

$$\begin{cases}
 F(\eta, T) \\
 = \frac{R_1}{2} \left[\frac{1}{k_1^2} \left(1 - \frac{\cosh E^{-\frac{1}{2}} k_1 \eta}{\cosh E^{-\frac{1}{2}} k_1} \right) e^{i\omega T} \right. \\
 \left. + \frac{1}{k_2^2} \left(1 - \frac{\cosh E^{-\frac{1}{2}} k_2 \eta}{\cosh E^{-\frac{1}{2}} k_2} \right) e^{-i\omega T} \right].
 \end{cases} \tag{28}$$

It may be noted that magnetic Reynolds number is very small in the case of vanishing magnetic Prandtl number P_m . Therefore, the induced magnetic field $b(\eta, T)$ produced by fluid motion is negligible in comparison to applied one (Cramer and Pai [30]).

When the frequency parameter ω is large and both Ekman number E and magnetic interaction parameter α_m^2

are small orders of magnitude, fluid flow becomes boundary layer type. For the boundary layer flow adjacent to the upper plate $\eta = 1$, introducing boundary layer coordinate $\xi = 1 - \eta$, the expression for fluid velocity (28) assumes the form

$$\begin{cases}
 u(\eta, T) = \frac{R_1}{\omega} \cos(\omega T - \frac{\Pi}{2}) \\
 - \frac{R_1}{2\omega} [e^{-\alpha_3 \xi} \sin(\omega T - \beta_3 \xi) \\
 + e^{-\alpha_4 \xi} \sin(\omega T - \beta_4 \xi)],
 \end{cases} \tag{29}$$

$$\begin{cases}
 v(\eta, T) = \frac{R_1}{2\omega} [e^{-\alpha_3 \xi} \cos(\omega T - \beta_3 \xi) \\
 - e^{-\alpha_4 \xi} \cos(\omega T - \beta_4 \xi)],
 \end{cases} \tag{30}$$

where

$$\begin{cases}
 \alpha_3 = (\frac{\omega}{2E})^{\frac{1}{2}} (1 + \frac{1}{\omega} + \frac{\alpha_m^2}{\omega}), \\
 \beta_3 = (\frac{\omega}{2E})^{\frac{1}{2}} (1 + \frac{1}{\omega} - \frac{\alpha_m^2}{\omega}), \\
 \alpha_4 = (\frac{\omega}{2E})^{\frac{1}{2}} (1 - \frac{1}{\omega} + \frac{\alpha_m^2}{\omega}), \\
 \beta_4 = (\frac{\omega}{2E})^{\frac{1}{2}} (1 - \frac{1}{\omega} - \frac{\alpha_m^2}{\omega}).
 \end{cases} \tag{31}$$

The expressions (29) and (30) reveal that fluid flow has three modes of oscillations. The first mode corresponds to pure oscillations of frequency ω which are due to applied pressure gradient and fill the entire fluid region. The other two modes of oscillations correspond to the modified hydromagnetic Stokes flow and are confined within double boundary layers of thickness $O(\frac{1}{\alpha_3})$ and $O(\frac{1}{\alpha_4})$. These boundary layers may be recognized as hydromagnetic Stokes-Ekman boundary layers. In the absence of magnetic field these boundary layers may be identified as Stokes-Ekman boundary layers. It is also evident from expressions in (31) that the thickness of these boundary layers decreases with increase in either magnetic interaction parameter α_m or frequency parameter ω or both whereas it increases with increase in Ekman number E . The exponential terms in the expressions (29) and (30) damp out quickly as ξ increases. When $\xi \geq \frac{1}{\alpha_4}$ i.e. outside the modified hydromagnetic Stokes-Ekman boundary layer region, we obtain

$$u \approx \frac{R_1}{\omega} \cos(\omega T - \frac{\Pi}{2}), v \approx 0. \tag{32}$$

It is observed from (32) that in the central core, given by $\xi \geq \frac{1}{\alpha_4}$ about the axis of the channel, the secondary velocity vanishes away while the primary velocity persists and has phase lag of $\frac{\Pi}{2}$ over it.

It is appropriate to mention here that in the limit of $P_m \rightarrow 0$, m_1 and m_2 become zero which implies that for large ω the thickness of m_1 and m_2 boundary layers, which may be recognized as magnetic diffusion boundary layers, tends to infinity implying thereby that the magnetic diffusion region extends up to the central line of

the channel as it happens in the limit $\omega \rightarrow 0$ and $P_m \neq 0$.

Case-II: The Case of Small Finite Magnetic Prandtl Number (*i.e.* $0 < P_m < 1$)

It is noticed from Case-I that in the limit $P_m \rightarrow 0$ and for large ω the flow-field is divided into two regions, namely, (i) hydromagnetic Stokes-Ekman layer region and (ii) the spatially and temporally uniform region beyond hydromagnetic Stokes-Ekman layer region *i.e.* magnetic diffusion region. Now we consider more realistic (but less tractable) situation in which magnetic Prandtl number P_m is still smaller than unity but greater than zero. From Case-I it is also evident that magnetic diffusion region (MDR) is always thicker than hydromagnetic Stokes-Ekman layer region. Therefore, for case of interest MDR should be relatively inviscid. The basis for an approximation valid within the MDR could now be the inviscid approximation to m_1 and m_2 itself (Benton and Loper [34]) which can be found from the inviscid version of the equations (19) to (23) as

$$\begin{cases} m_1 = m_{11} = i \left[\frac{\omega P_m (\omega + 2)}{2\alpha_m^2 + i(\omega + 2)} \right]^{\frac{1}{2}}, \\ m_2 = m_{22} = i \left[\frac{\omega P_m (\omega - 2)}{2\alpha_m^2 - i(\omega - 2)} \right]^{\frac{1}{2}}. \end{cases} \quad (33)$$

Now expanding full expression for $k_{1,2}$ and $m_{1,2}$ in the expressions (26) in power of $P_m^{\frac{1}{2}}$, we obtain

$$\begin{cases} k_1 = [2\alpha_m^2 + i(\omega + 2)]^{\frac{1}{2}} \\ \quad \times [1 + \phi_1(P_m) + O(P_m^2)] \\ \quad = k_{11}[1 + \phi_1 + O(P_m^2)], \\ k_2 = [2\alpha_m^2 - i(\omega - 2)]^{\frac{1}{2}} \\ \quad \times [1 - \phi_2(P_m) + O(P_m^2)] \\ \quad = k_{22}[1 - \phi_2 + O(P_m^2)], \\ m_1 = i \left[\frac{\omega P_m (\omega + 2)}{2\alpha_m^2 + i(\omega + 2)} \right]^{\frac{1}{2}} \\ \quad \times [1 - \phi_1(P_m) + O(P_m^2)] \\ \quad = m_{11}[1 - \phi_1 + O(P_m^2)], \\ m_2 = i \left[\frac{\omega P_m (\omega - 2)}{2\alpha_m^2 - i(\omega - 2)} \right]^{\frac{1}{2}} \\ \quad \times [1 + \phi_2(P_m) + O(P_m^2)] \\ \quad = m_{22}[1 + \phi_2 + O(P_m^2)], \end{cases} \quad (34)$$

where

$$\begin{cases} \phi_1 = \frac{P_m(i\omega\alpha_m^2)}{\{2\alpha_m^2 + i(\omega + 2)\}^2}, \\ \phi_2 = \frac{P_m(i\omega\alpha_m^2)}{\{2\alpha_m^2 - i(\omega - 2)\}^2}. \end{cases} \quad (35)$$

The expressions of $k_{1,2}$ and $m_{1,2}$ are substituted in the equations (24) and (25) and coefficient function in these equations are expanded in powers of $P_m^{\frac{1}{2}}$. When terms only up to order $P_m^{\frac{1}{2}}$ are retained, the resulting solution for velocity and induced magnetic field are expressed in the

following form

$$\begin{cases} F(\eta, T) = -\frac{i}{2(\omega + 2)} [R_1 \{C_{11} (\cosh \alpha_{11} \eta \\ - \frac{\cosh \alpha_{11}}{\cosh \alpha_{22}} \cosh \alpha_{22} \eta) + (1 - \frac{\cosh \alpha_{22} \eta}{\cosh \alpha_{22}}) \\ + RC_{22} (\sinh \alpha_{11} \eta \\ - \frac{\sinh \alpha_{11}}{\sinh \alpha_{22}} \sinh \alpha_{22} \eta)\} e^{i\omega T} \\ + \frac{i}{2(\omega - 2)} [R_1 \{a_{11} (\cosh \beta_{11} \eta \\ - \frac{\cosh \beta_{11}}{\cosh \beta_{22}} \cosh \beta_{22} \eta) + (1 - \frac{\cosh \beta_{22} \eta}{\cosh \beta_{22}}) \\ + Ra_{22} (\sinh \beta_{11} \eta \\ - \frac{\sinh \beta_{11}}{\sinh \beta_{22}} \sinh \beta_{22} \eta)\} e^{-i\omega T}, \end{cases} \quad (36)$$

$$\begin{cases} b(\eta, T) = -\frac{m_{11}(m_{11}^2 - k_{11}^2)}{4\omega(\omega + 2)P_m\alpha_m^2} \\ \quad \times [R_1(C_{11} \cosh \alpha_{11} + 1) \frac{\sinh \alpha_{22} \eta}{\cosh \alpha_{22}} \\ + RC_{22} \frac{\sinh \alpha_{11}}{\sinh \alpha_{22}} \cosh \alpha_{22} \eta] e^{i\omega T} \\ - \frac{m_{22}(m_{22}^2 - k_{22}^2)}{4\omega(\omega - 2)P_m\alpha_m^2} \\ \quad \times [R_1(a_{11} \cosh \beta_{11} + 1) \frac{\sinh \beta_{22} \eta}{\cosh \beta_{22}} \\ + Ra_{22} \frac{\sinh \beta_{11}}{\sinh \beta_{22}} \cosh \beta_{22} \eta] e^{-i\omega T}, \end{cases} \quad (37)$$

where

$$\begin{cases} \alpha_{11}, \alpha_{22} = E^{-\frac{1}{2}}(k_{11}, m_{11}), \\ \beta_{11}, \beta_{22} = E^{-\frac{1}{2}}(k_{22}, m_{22}), \\ C_{11} = -\sec h \alpha_{11}, \\ C_{22} = \frac{2\omega(\omega + 2)P_m\alpha_m^2}{m_{11}(m_{11}^2 - k_{11}^2) \sinh \alpha_{11} \coth \alpha_{22}}, \\ a_{11} = -\sec h \beta_{11}, \\ a_2 = \frac{2\omega(\omega - 2)P_m\alpha_m^2}{m_{22}(m_{22}^2 - k_{22}^2) \sinh \beta_{11} \coth \beta_{22}}. \end{cases} \quad (38)$$

When ω is large and E and α_m^2 are of small orders of magnitude, the fluid flow represents boundary layer type flow. For the boundary layer flow near the upper plate $\eta = 1$, introducing boundary layer coordinate $\xi = 1 - \eta$, the expressions for fluid velocity and induced magnetic field, obtained from (36) to (38), are presented in the following form

$$\begin{cases} u(\eta, T) = \frac{R_1}{\omega} \cos(\omega T - \frac{\Pi}{2}) \\ - e^{-\alpha_3 \xi} [R(\frac{P_m}{2\omega})^{1/2} \alpha_m^2 (1 - \frac{2}{\omega}) \\ \quad \times \{ \cos(\omega T - \beta_3 \xi) + \sin(\omega T - \beta_3 \xi) \} \\ + \frac{R_1}{2\omega} \sin(\omega T - \beta_3 \xi)] \\ + e^{-\alpha_4 \xi} [R(\frac{P_m}{2\omega})^{1/2} \alpha_m^2 (1 + \frac{2}{\omega}) \\ \quad \times \{ \cos(\omega T - \beta_4 \xi) + \sin(\omega T - \beta_4 \xi) \} \\ - \frac{R_1}{2\omega} \sin(\omega T - \beta_4 \xi)] \\ - \frac{4R}{2\omega} (\frac{P_m}{2\omega})^{1/2} \alpha_m^2 e^{-\alpha_5 \xi} \\ \quad \times [\cos(\omega T - \beta_5 \xi) + \sin(\omega T - \beta_5 \xi)], \end{cases} \quad (39)$$

$$\begin{cases}
 v(\eta, T) = e^{-\alpha_3 \xi} [R(\frac{P_m}{2\omega})^{1/2} \alpha_m^2 \\
 \times (1 - \frac{2}{\omega}) \{ \cos(\omega T - \beta_3 \xi) \\
 - \sin(\omega T - \beta_3 \xi) \} \\
 + \frac{R_1}{2\omega} \cos(\omega T - \beta_3 \xi) \\
 + e^{-\alpha_4 \xi} [R(\frac{P_m}{2\omega})^{1/2} \alpha_m^2 (1 - \frac{2}{\omega}) \\
 \{ \cos(\omega T - \beta_3 \xi) - \sin(\omega T - \beta_3 \xi) \} \\
 - \frac{R_1}{2\omega} \cos(\omega T - \beta_3 \xi)] - 2R(\frac{P_m}{2\omega})^{1/2} \alpha_m^2 \\
 \times e^{-\alpha_5 \xi} [\cos(\omega T - \beta_5 \xi) \\
 - \sin(\omega T - \beta_5 \xi)],
 \end{cases} \quad (40)$$

$$B_x = Re^{-\alpha_5 \xi} \cos(\omega T - \beta_5 \xi), \quad B_y = 0, \quad (41)$$

where

$$\begin{cases}
 \alpha_5 = (\frac{\omega P_m}{2E})^{1/2} (1 - \frac{\alpha_m^2}{\omega}), \\
 \beta_5 = (\frac{\omega P_m}{2E})^{1/2} (1 + \frac{\alpha_m^2}{\omega}).
 \end{cases} \quad (42)$$

The expressions (39) to (42) reveal that the oscillatory flow has four modes of oscillations. The first mode corresponds to pure oscillations of frequency ω due to applied oscillatory pressure gradient which persist into entire fluid region. The other three modes correspond to the modified hydromagnetic Stokes flow and are confined within triple boundary layers of thickness $O(\frac{1}{\alpha_3})$, $O(\frac{1}{\alpha_4})$ and $O(\frac{1}{\alpha_5})$. Two of the layers of thickness $O(\frac{1}{\alpha_3})$ and $O(\frac{1}{\alpha_4})$ may be identified as modified hydromagnetic Stokes-Ekman boundary layer similar to that of Case-I.

Since the magnetic interaction parameter α_m^2 is independent of viscosity and it is noted from the expressions in (42) that α_5 is independent of viscosity and depending instead only on the magnetic diffusivity or resistivity. Henceforth, it is referred as an inviscid magnetic diffusion boundary layer or magnetic diffusion region of thickness $O(\frac{1}{\alpha_5})$ and it is thicker than hydromagnetic Stokes-Ekman layer region. The thickness of this region increases with increase in either α_m^2 or E or both. The exponential terms in the equations (39) and (40) damp out quickly as ξ increases.

When $\xi \geq 1/\alpha_5$, we obtain

$$\begin{cases}
 u \approx \frac{R_1}{\omega} \cos(\omega T - \Pi/2), \quad v \approx 0, \\
 B_x \approx 0, \quad B_y \approx 0.
 \end{cases} \quad (43)$$

It is evident from (43) that the central core, given by $\xi \geq \frac{1}{\alpha_5}$ about the axis of the channel i.e. outside the hydromagnetic Stokes-Ekman layer region and magnetic diffusion region, is a current free zone in which fluid has a velocity in the primary flow direction and it oscillates with the same frequency ω as the pressure gradient but has a phase lag of $\frac{\Pi}{2}$ over it.

It is observed in Cases-I and II that the main difference between the flow when $P_m \rightarrow 0$ and $0 < P_m < 1$ is that, in the latter case magnetic diffusion region has a finite thickness $O(\frac{1}{\alpha_5})$ and also there is a

third region of flow, that beyond both hydromagnetic Stokes-Ekman layer region and magnetic diffusion region. This outer most region i.e. central core region is called current free region which extends up to the central line of the channel. However, in the former case there exist two regions only, namely, hydromagnetic Stokes-Ekman layer region and magnetic diffusion region extending up to the central line of the channel.

3 Shear stress at the plates

The non-dimensional shear stress components τ_x and τ_y at both the upper and lower plates $\eta = \pm 1$ due to primary and secondary flows respectively, are given by

$$\begin{cases}
 (\tau_x + i\tau_y)_{\eta \pm 1} = -\frac{i}{2(\omega+2)} \\
 \times [\pm R_1 \{ C_1(\alpha_1 \sinh \alpha_1 \\
 - \alpha_2 \cosh \alpha_1 \tanh \alpha_2) - \alpha_2 \tanh \alpha_2 \} \\
 + RC_2(\alpha_1 \cosh \alpha_1 - \alpha_2 \coth \alpha_2)] e^{i\omega T} \\
 + \frac{i}{2(\omega-2)} [\pm R_1 \{ a_1(\beta_1 \sinh \beta_1 \\
 - \beta_2 \cosh \beta_1 \tanh \beta_2) - \beta_2 \tanh \beta_2 \} \\
 + Ra_2(\beta_1 \cosh \beta_1 \\
 - \beta_2 \sinh \beta_1 \coth \beta_2)] e^{-i\omega T}.
 \end{cases} \quad (44)$$

4 Mass flow rate

The expression for non-dimensional mass flow rates Q_x and Q_y , due to primary and secondary flows respectively, is given by

$$\begin{cases}
 Q_x + iQ_y = -\frac{iR_1}{(\omega+2)} [C_1(\frac{\sinh \alpha_1}{\alpha_1} \\
 - \frac{\cosh \alpha_1 \tanh \alpha_2}{\alpha_2}) + (1 - \frac{\tanh \alpha_2}{\alpha_2})] e^{i\omega T} \\
 + \frac{iR_1}{(\omega-2)} [a_1(\frac{\sinh \beta_1}{\beta_1} - \frac{\cosh \beta_1 \tanh \beta_2}{\beta_2}) \\
 + (1 - \frac{\tanh \beta_2}{\beta_2})] e^{-i\omega T}.
 \end{cases} \quad (45)$$

5 Results and discussion

To study the effects of oscillations and magnetic field on the flow-field, the numerical values of both the primary and secondary fluid velocities and primary and secondary induced magnetic fields, computed from the analytical solution (24) to (26), are displayed graphically versus channel width variable η in figures-2 to 9 for various values of frequency parameter ω and magnetic interaction parameter α_m^2 taking Ekman number $E = 0.04$, magnetic Prandtl number $P_m = 0.7$ (i.e. ionized hydrogen), $R = R_1 = 1$ and $\omega T = \frac{\pi}{2}$. Figures-2 and 3 illustrate the influence of oscillations on the primary velocity u and secondary velocity v . It is evident from figures-2 and 3 that the primary velocity u increases on increasing ω near the lower and upper plates of the channel and is of oscillatory character in the region $0.17 \leq \eta \leq 0.47$. Secondary velocity v decreases on increasing ω in the

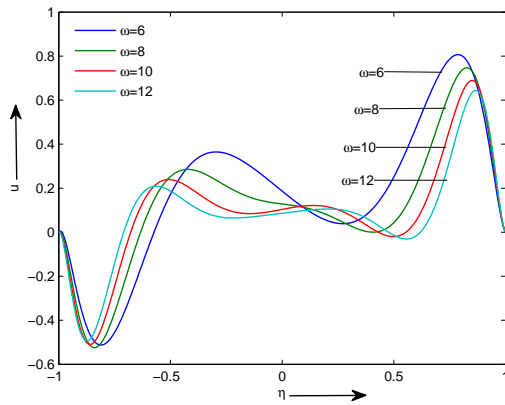


Fig. 2: Primary velocity profiles when $\alpha_m^2 = 5$

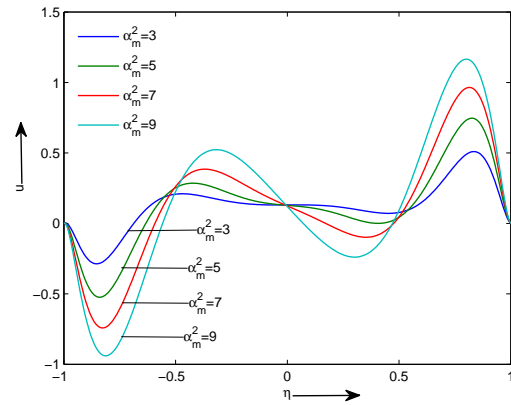


Fig. 4: Primary velocity profiles when $\omega = 8$

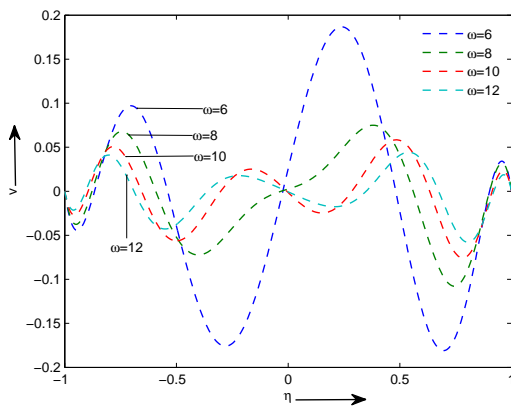


Fig. 3: Secondary velocity profiles when $\alpha_m^2 = 5$

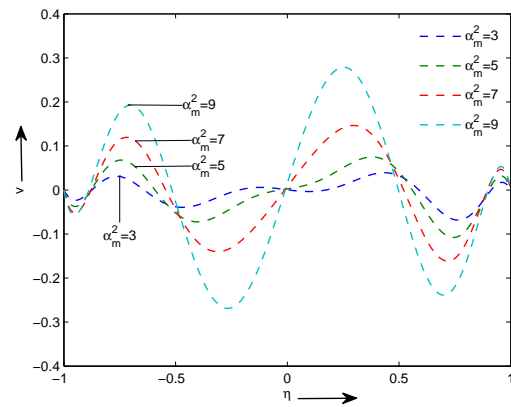


Fig. 5: Secondary velocity profiles when $\omega = 8$

regions $-1 \leq \eta \leq -0.5$ and $0.5 \leq \eta \leq 1$ and it is of oscillatory nature in the central region of the channel. This implies that oscillations tend to accelerate fluid flow in the primary flow direction near the lower and upper plates of the channel whereas it has reverse effect on the fluid flow in the secondary flow direction the regions $-1 \leq \eta \leq -0.5$ and $0.5 \leq \eta \leq 1$.

Figures-4 and 5 depict the effects of magnetic field on the primary velocity u and secondary velocity v . It is revealed from figures-4 and 5 that both the primary velocity u and the secondary velocity v increase on increasing α_m^2 throughout the channel. This implies that magnetic field tends to accelerate fluid flow in both the primary and secondary flow directions throughout the channel. It may be noted that from figures-2 to 4 that there exists reverse flow in both the primary and secondary flow directions on increasing either ω or α_m^2 .

Figures-6 and 7 show the effects of oscillations on the primary induced magnetic field B_x and secondary induced

magnetic field B_y . It is seen from figures-6 and 7 that the primary induced magnetic field B_x increases on increasing ω near the lower and upper plates of the channel and is of oscillatory nature in the region $-0.5 \leq \eta \leq 0.5$. Secondary induced magnetic field B_y decreases on increasing ω near the lower and upper plates of the channel and it is of oscillatory character in the region $-0.7 \leq \eta \leq 0.7$. This implies that oscillations tends to enhance induced magnetic field in the primary flow direction whereas it has reverse effect on the induced magnetic field in the secondary flow direction near the lower and upper plates of the channel.

Figures-8 and 9 exhibit the influence of magnetic field on the primary induced magnetic field B_x and secondary induced magnetic field B_y . It is observed from figures-8 and 9 that the primary induced magnetic field B_x increases on increasing α_m^2 the lower and upper plates of the channel and is of oscillatory nature in the region $-0.57 \leq \eta \leq 0.57$. Secondary induced magnetic field B_y increases on increasing α_m^2 near the lower and upper

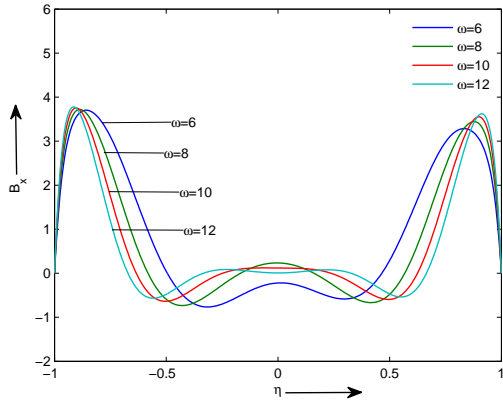


Fig. 6: Primary induced magnetic field profiles when $\alpha_m^2 = 5$

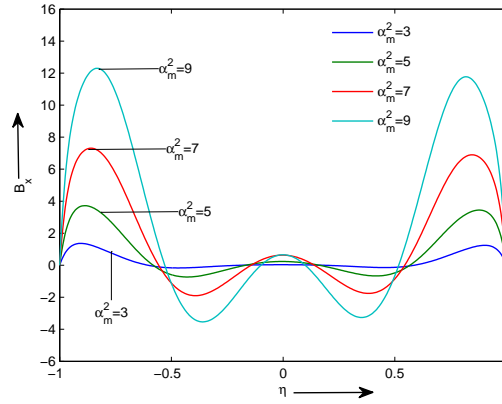


Fig. 8: Primary induced magnetic field profiles when $\omega = 8$

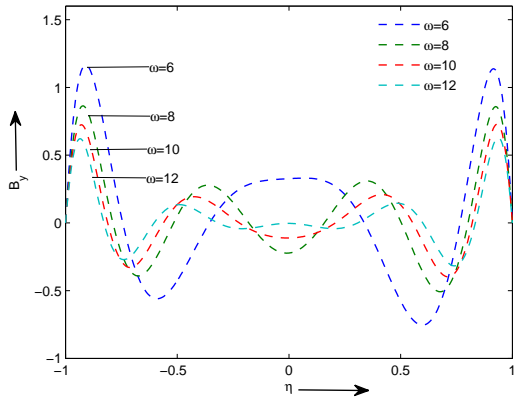


Fig. 7: Secondary induced magnetic field profiles when $\alpha_m^2 = 5$

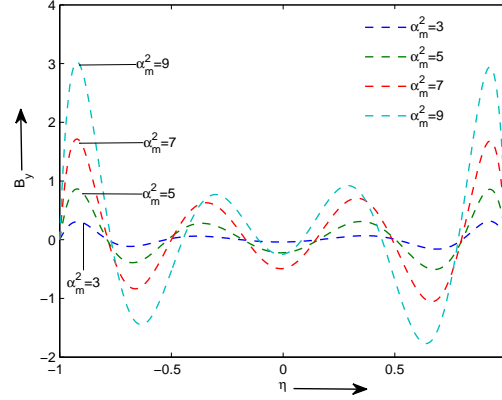


Fig. 9: Secondary induced magnetic field profiles when $\omega = 8$

plates of the channel and it is of oscillatory character in the region $-0.8 \leq \eta \leq 0.8$. This implies that magnetic field tends to enhance induced magnetic field in both the primary and secondary flow directions near the lower and upper plates of the channel.

The numerical values of the primary shear stress τ_x and secondary shear stress τ_y at the lower and upper plates of the channel, computed from the analytical expression (44), are displayed in tabular form in tables-1 and 2 while that of mass flow rate in the primary flow direction Q_x and mass flow rate in the secondary flow direction Q_y , computed from analytical expression (45), are presented in tabular form in table-3 for various values of ω and α_m^2 . It is revealed from table-1 that the primary shear stress at the lower plate $(\tau_x)_{\eta=-1}$ decreases on increasing ω whereas it increases on increasing α_m^2 when $\omega \geq 8$ and it increases, attains a maximum and then decreases on increasing α_m^2 when $\omega = 6$. Secondary shear stress at the lower plate $(\tau_y)_{\eta=-1}$ increases on increasing α_m^2 whereas it decreases on increasing ω except when

$\alpha_m^2 = 7$. For $\alpha_m^2 = 7$, it increases, attains a maximum and then decreases on increasing ω . This implies that oscillations have tendency to reduce primary shear stress and also secondary shear stress except when $\alpha_m^2 = 7$ at the lower plate of the channel. Magnetic field tends to enhance primary shear stress when $\omega \geq 8$ and secondary shear stress at the lower plate of the channel. It is observed from table-2 that both the primary shear stress at the upper plate $(\tau_x)_{\eta=1}$ and secondary shear stress at the upper plate $(\tau_y)_{\eta=1}$ increase on increasing α_m^2 . Primary shear stress at the upper plate $(\tau_x)_{\eta=1}$ decreases on increasing ω whereas secondary shear stress at the upper plate $(\tau_y)_{\eta=1}$ decreases on increasing ω when $\alpha_m^2 \leq 5$ and it increases, attains a maximum and then decreases on increasing ω when $\alpha_m^2 = 7$ and 9. This implies that magnetic field tends to enhance both the primary and secondary shear stress at the upper plate of the channel. Oscillations tend to reduce primary shear stress and secondary shear stress when $\alpha_m^2 \leq 5$ at the upper plate of the channel. It is evident from table-3 that mass flow rates

in the primary flow direction Q_x and mass flow rate in the secondary flow direction Q_y decrease on increasing ω . Mass flow rate in the secondary flow direction Q_y increases on increasing α_m^2 whereas mass flow rate in the primary flow direction Q_x increases on increasing α_m^2 when $\omega \geq 8$ and it increases, attains a maximum and then decreases on increasing α_m^2 when $\omega = 6$. This implies that oscillations tend reduce the mass flow rate in both the primary and secondary flow directions. Magnetic field tends to enhance mass flow rate in the primary flow direction when $\omega \geq 8$ and mass flow rate in the secondary flow direction.

Table-1: Primary and secondary shear stress at the lower plate

$\alpha_m^2 \downarrow \omega \rightarrow$	$(\tau_x)_{\eta=-1}$				$-(\tau_y)_{\eta=-1}$			
	6	8	10	12	6	8	10	12
3	1.4894	1.2591	1.1226	1.0216	1.1817	0.9803	0.8207	0.7086
5	1.7054	1.3321	1.1884	1.0700	1.7801	1.6519	1.3599	1.1751
7	1.9299	1.3979	1.2588	1.1194	2.1504	2.3315	1.9235	1.6321
9	1.8844	1.4751	1.3394	1.1696	3.0384	2.7161	2.6056	2.0673

Table-2: Primary and secondary shear stress at the upper plate

$\alpha_m^2 \downarrow \omega \rightarrow$	$(\tau_x)_{\eta=1}$				$-(\tau_y)_{\eta=1}$			
	6	8	10	12	6	8	10	12
3	1.4754	1.2634	1.1216	1.0217	1.1323	0.9581	0.8076	0.7005
5	1.5468	1.3637	1.1821	1.0705	1.7254	1.6426	1.3510	1.1704
7	1.5933	1.4797	1.2398	1.1209	2.0048	2.3481	1.9161	1.6302
9	1.8350	1.6007	1.2855	1.1727	2.7005	2.7748	2.5994	2.0663

Table-3: Mass flow rates in primary and secondary flow directions

$\alpha_m^2 \downarrow \omega \rightarrow$	Q_x				$-Q_y$			
	6	8	10	12	6	8	10	12
3	0.3470	0.2508	0.1977	0.1636	0.0232	0.0098	0.0053	0.0032
5	0.3488	0.2519	0.1983	0.1640	0.0260	0.0105	0.0056	0.0034
7	0.3492	0.2530	0.1988	0.1643	0.0289	0.0113	0.0059	0.0036
9	0.3482	0.2541	0.1993	0.1646	0.0298	0.0124	0.0062	0.0037

6 Conclusions

A mathematical analysis has been presented for oscillatory Hartmann flow of a viscous, incompressible and electrically conducting fluid in a rotating channel with magnetized walls in the presence of a uniform transverse magnetic field. The significant results are summarized below:

Oscillations tend to accelerate fluid flow in the primary flow direction near the lower and upper plates of the channel whereas it has reverse effect on the fluid flow in the secondary flow direction the regions $-1 \leq \eta \leq -0.5$ and $0.5 \leq \eta \leq 1$. Magnetic field tends to accelerate fluid flow in both the primary and secondary flow directions throughout the channel. Oscillations tends to enhance induced magnetic field in the primary flow direction whereas it has reverse effect on the induced

magnetic field in the secondary flow direction near the lower and upper plates of the channel. Magnetic field tends to enhance induced magnetic field in both the primary and secondary flow directions near the lower and upper plates of the channel.

Oscillations have tendency to reduce primary shear stress and also secondary shear stress except when $\alpha_m^2 = 7$ at the lower plate of the channel. Magnetic field tends to enhance primary shear stress when $\omega \geq 8$ and secondary shear stress at the lower plate of the channel. Magnetic field tends to enhance both the primary and secondary shear stress at the upper plate of the channel. Oscillations tend to reduce primary shear stress and secondary shear stress when $\alpha_m^2 \leq 5$ at the upper plate of the channel. Oscillations tend reduce the mass flow rate in both the primary and secondary flow directions. Magnetic field tends to enhance mass flow rate in the primary flow direction when $\omega \geq 8$ and mass flow rate in the secondary flow direction.

References

- [1] R. Hide, P. H. Roberts, *Hydromagnetic flow due to an oscillating plane*, Reviews of Modern Physics **32**, 799–806 (1960).
- [2] R. S. Nanda, H. K. Mohanty, *Hydromagnetic flow in a rotating channel*, Appl. Sci. Res. **24**, 65–78 (1971).
- [3] A. S. Gupta, *Magnetohydrodynamic Ekman layer*, Acta Mechanica **13**, 155–160 (1972).
- [4] D. J. Acheson, *Forced hydromagnetic oscillations of a rapidly rotating fluid*, Physics of Fluids **18**, 961–968 (1975).
- [5] G. S. Seth, R. N. Jana, *Unsteady hydromagnetic flow in a rotating channel with oscillating pressure gradient*, Acta Mechanica **37**, 29–41 (1980).
- [6] G. Sarojamma, D. V. Krishna, *Transient hydromagnetic convective flow in a rotating channel with porous boundaries*, Acta Mechanica **40**, 277–288 (1981).
- [7] G. S. Seth, R. N. Jana, M. K. Maiti, *Unsteady hydromagnetic Couette flow in a rotating system*, Int. J. Engng. Sci. **20**, 989–999 (1982).
- [8] G. S. Seth, R. Singh, N. Mahato, *Oscillatory hydromagnetic Couette flow in a rotating system*, Ind. J. Tech. **26**, 329–333 (1988).
- [9] G. S. Seth, R. Nandkeolyar, Md. S. Ansari, *Hall effects on oscillatory hydromagnetic Couette flow in a rotating system*, Int. J. Acad. Res. **1(2)**, 6–17 (2009).
- [10] G. S. Seth, Md. S. Ansari, R. Nandkeolyar, *Unsteady hydromagnetic Couette flow within porous plates in a rotating system*, Adv. Appl. Math. Mech. **2(3)**, 286–302 (2010).
- [11] G. S. Seth, Md. S. Ansari, R. Nandkeolyar, *Unsteady hydromagnetic Couette flow induced due to accelerated movement of one of the porous plates of the channel in a rotating system*, Int. J. Appl. Math. Mech. **6(7)**, 24–42 (2010).
- [12] G. S. Seth, Md. S. Ansari, R. Nandkeolyar, *Effects of rotation and magnetic field on unsteady Couette flow in a porous channel*, J. Appl. Fluid Mech. **4(2)**, 95–103 (2011).

- [13] G. S. Seth, S. K. Ghosh, *Unsteady hydromagnetic flow in a rotating channel in the presence of oblique magnetic field*, Int. J. Engng. Sci. **24**, 1183–1193 (1986).
- [14] A. Raptis, A. K. Singh, *Hydromagnetic Rayleigh problem in a rotating fluid*, Acta Physica Hungarica **60**, 221–226 (1986).
- [15] N. Nanousis, *Thermal-Diffusion on MHD free-convection and mass transfer flow past a moving infinite vertical plate in a rotating fluid*, Astrophysics and Space Science **191**, 313–322 (1992).
- [16] P. Chandran, N. C. Sacheti, A. K. Singh, *Effect of rotation on unsteady hydromagnetic Couette flow*, Astrophysics and Space Science **202**, 1–10 (1993).
- [17] A. K. Singh, N. C. Sacheti, P. Chandran, *Transient effects on Magnetohydrodynamic Couette flow with rotation: Accelerated motion*, Int. J. Engng. Sci. **32**, 133–139 (1994).
- [18] T. Nagy, Z. Demendy, *Effects of Hall currents and Coriolis force on Hartmann flow under general wall conditions*, Acta Mechanica **113**, 77–91 (1995).
- [19] K. D. Singh, *An oscillatory hydromagnetic Couette flow in a rotating system*, ZAMM **80**, 429–432 (2000).
- [20] T. Hayat, S. Nadeem, S. Asghar, *Hydromagnetic Couette flow of a Oldroyd-B fluid in a rotating system*, Int. J. Engng. Sci. **42**, 65–78 (2004).
- [21] T. Hayat, S. Nadeem, A. M. Siddiqui, S. Asghar, *An oscillatory hydromagnetic Non-Newtonian flow in a rotating system*, Appl. Math. Lett. **17**, 609–614 (2004).
- [22] T. Hayat, K. Hutter, S. Nadeem, S. Asghar, *Unsteady hydromagnetic rotating flow of a conducting second grade fluid*, ZAMP **55**, 626–641 (2004).
- [23] T. Hayat, S. B. Khan, M. Khan, *Exact solution for rotating flows of a generalized Burgers fluid in a porous space*, Appl. Math. Model. **32**, 749–760 (2008).
- [24] S. K. Ghosh, I. Pop, *Hall effects on MHD plasma Couette flow in a rotating environment*, Int. J. Appl. Mech. Eng. **9**, 293–305 (2004).
- [25] S. K. Ghosh, I. Pop, *An analytical approach on MHD plasma behavior of rotating environment in the presence of an inclined magnetic field as compared to excitation frequency*, Int. J. Appl. Mech. Eng. **11**, 845–856 (2006).
- [26] S. K. Ghosh, O. A. Beg, M. Narahari, *Hall effects on MHD flow in a rotating system with heat transfer characteristics*, Mecannica **44**, 741–765 (2009).
- [27] M. Guria, S. Das, R. N. Jana, S. K. Ghosh, *Oscillatory Couette flow in the presence of inclined magnetic field*, Mecannica **44**, 555–564 (2009).
- [28] S. Das, S. L. Maji, M. Guria, R. N. Jana, *Unsteady MHD Couette flow in a rotating system*, Math. Comp. Model. **50**, 1211–1217 (2009).
- [29] D. S. Chauhan, R. Agrawal, *Effects of Hall current on MHD Couette flow in a channel partially filled with porous medium in a rotating system*, Meccanica **47**, 405–421 (2012).
- [30] K. R. Cramer, S. I. Pai, *Magneto-fluid-dynamics for Engineers and Applied Physicists*, McGraw Hill Book Company, New York (1973).
- [31] S. K. Ghosh, *Unsteady hydromagnetic flow in a rotating channel with oscillating pressure gradient*, J. Phy. Soc. Japan **62**, 3893–3903 (1993).
- [32] G. S. Seth, Md. S. Ansari, R. Nandkeolyar, *Unsteady Hartmann flow in a rotating channel with perfectly conducting walls*, Int. J. Appl. Mech. Eng. **16(4)**, 1129–1146 (2011).
- [33] Md. S. Ansari, G. S. Seth, R. Nandkeolyar, *Unsteady Hartmann flow in a rotating channel with arbitrary conducting walls*, Math. Comp. Model. **54**, 765–779 (2011).
- [34] E. R. Benton, D. E. Loper, *On the spin up of an electrically conducting fluid Part I. The unsteady hydromagnetic Ekman-Hartmann boundary layer problem*, J. Fluid Mech. **39**, 561–586 (1969).



G. S. Seth is a Professor in the Department of Applied Mathematics, Indian School of Mines, Dhanbad, INDIA. He received his Ph. D. in the Mathematics from Indian Institute of Technology, Kharagpur, India. He has more than thirty four years of experience of teaching and research. His current area of research studies includes Fluid dynamics, Magnetohydrodynamics and heat and mass transfer. He was visiting Assistant Professor at University of Aden, Republic of Yemen during the period September 01, 1991 to August 31, 1993. He has published more than one hundred fifteen research papers in national/International journals of repute.



J. K. Singh is Assistant Professor in Department of Studies in Mathematics, V. S. K. University, Bellary, INDIA. He has receive Ph.D. in Applied Mathematics from Indian School of Mines, Dhanbad, INDIA. He has published a number of reseach papers in international journals of repute. His research areas are Fluid Mechanics, MHD and Numerical Analysis.



N. Mahto is an Associate Professor in the Department of Mathematics, RSP College Jharia, Vinobha Bhawe Univeristy, Hazaribagh, Jharkhand, INDIA. He received his Ph. D. in Applied Mathematics from Indian School of Mines, Dhanbad, India. He has more than thirty three years of teaching experience and more than twenty three years of research experience. His current area of research studies includes Fluid dynamics, Magnetohydrodynamics and heat and mass transfer. He has published more than fifteen research papers in national/International journals of repute.



N.
Joshi is doing research work leading to Ph. D. degree in Department of Mathematics, V. S. K. University, Bellary, INDIA. His research areas are Fluid Mechanics, MHD and Numerical Analysis.